The Coldest Object in the Universe: Probing the Mass Distribution of the Ultra-Cold Outf ow and Dusty Disk in the Boomerang Nebula

R. Sahai[1], W. Vlemmings[2], and L-Å Nyman[3]

[1]*Jet Propulsion Laboratory, California Institue of Technology, Pasadena, CA 91109, USA* sahai@jpl.nasa.gov

[2]*Chalmers University of Technology, Onsala Space Observatory, 439 92 Onsala, Sweden* wouter.vlemmings@chalmers.se

[3]*Joint ALMA Observatory (JAO) and European Southern Observatory (ESO), Alonso de Cordova 3107, Vitacura, Santiago de Chile* lnyman@alma.cl

Abstract. Our Cycle 0 ALMA observations conf rmed that the Boomerang Nebula is the coldest known object in the Universe, with a massive high-speed outf ow that has cooled signif cantly below the temperature of the cosmic background (CMB). The Boomerang's prodigious mass-loss rate ($0.001\,M_\odot$ yr^{-1}) and low-luminosity ($300L_\odot$) make it a key object for understanding the remarkable transition of the circumstellar envelopes of AGB stars into bipolar planetary nebulae.

We have obtained new ACA CO 1-0 data that recover much of the f ux lost in the Cycle 0 data, and reveal heretofore unseen distant regions of the ultra-cold outf ow re-heated to temperatures above the CMB. Our CO J=3-2 data reveal the precise, highly collimated shape of an inner bipolar structure and its dense central waist, with unprecedented angular resolution (0.4″). The waist shows a core-halo structure in the thermal dust emission at 0.88 mm, and its derived f ux at this wavelength, compared with the 3.3, 2.6, and 1.3 mm f uxes support the presence of about $5 \times 10^{-4}\,M_\odot$of very large (~mm-sized), cold (~30K) grains. We also f nd the unexpected presence of weak SO emission, possibly resulting from the release of S from grains due to high-speed shocks.

1. Introduction

The Boomerang Nebula is the **coldest** known object in the Universe (Sahai & Nyman 1997: SN97). It is a bipolar Pre-Planetary Nebula (PPN), and represents a short-lived (~ 1000 yr) transition phase during which Asymptotic Giant Branch (AGB) stars and their round circumstellar envelopes (CSEs) evolve into planetary nebulae (PNe) with a breathtaking variety of aspherical geometrical shapes and symmetries (e.g., Sahai et al. 2007, Sahai, Morris & Villar 2011). Optical imaging shows that the Boomerang has an hourglass morphology as seen in the light ref ected by dust grains.

Single dish CO(1–0) observations showed an extended high-speed outf ow in absorption against the microwave background, implying that the nebula has cooled to a temperature signif cantly below that of the cosmic background radiation (T_{bb} = 2.7 K) due to adiabatic expansion (SN97), but the structure of the outf ow was not properly resolved due to the large beam-size (45″). We mapped the Boomerang with ALMA in Cycle 0 in the CO 1–0 and 2–1 lines with 4.3″ and 2.2″ resolution, respectively

(Sahai et al. 2013: Pap1). We confirmed that the extended high-velocity envelope has ultra-cold temperatures below the CMB, and although patchy, shows no systematic departures from a roughly round shape, and the observed angular sizes of the inner and outer outflows are in reasonable agreement with the SN97 model. The inner outflow was found to have a bipolar shape with a dense central disk completely unlike the ultra-cold outflow. The disk shapes the illumination of the nebula as a whole and provides a natural explanation for the overall hourglass optical morphology. We discovered patchy emission around the ultra-cold outflow, as expected from eventual heating of the gas due to grain photoelectric heating.

2. Cycle 1 ALMA Observations

2.1. Line Observations

We observed the CO(1–0) line towards the Boomerang with the 12m array (mosaic) and the 7m ACA. The CO(1-0) mapping recovers much of the flux lost in the Cycle 0 data (although up to $\gtrsim$50% of the flux is still resolved out at expansion speeds $\lesssim$70km s^{-1}), and reveals previously unseen distant regions (to a radius $\gtrsim$ 55″) of the ultra-cold outflow partially re-heated to temperatures above the CMB (Fig. 1) (however, total-power data are still needed to recover the full single-dish flux as seen by SN97). Taking the SN97 value of the mass-loss rate (1.3×10^{-3} $M_\odot$ yr^{-1}) for the ultracold outflow, we estimate a total ejecta mass of $\gtrsim$ 3 $M_\odot$ in the latter.

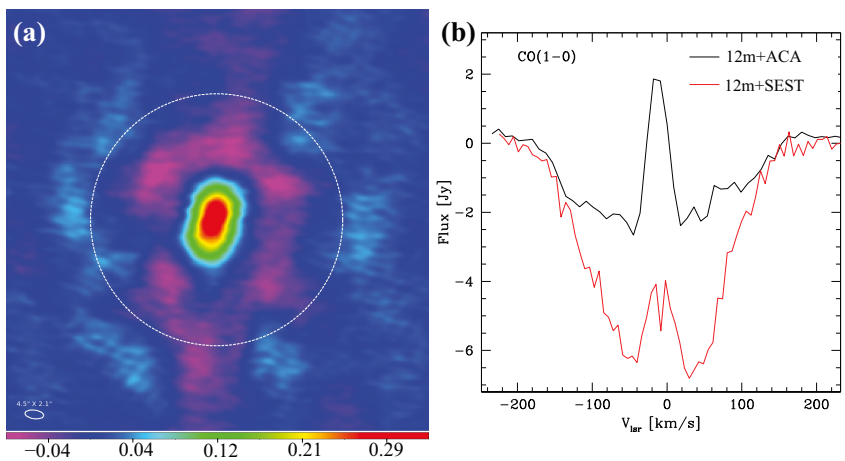

Figure 1. (a) ACA CO J=1-0 map of the Boomerang near its systemic velocity (color scale shows intensity in Jy/beam; beam is 4.5″ × 2.1″). The dotted white circle (diameter=100″) shows the region mapped in Cycle 0, (b) the total CO(1–0) flux extracted from the 12m+SEST image and the 12m+ACA image.

The J=3–2 line of both CO and ^{13}CO were observed with the 12m array. Our CO J=3-2 data show the precise, highly collimated shape of an inner bipolar structure and its dense central waist, with unprecedented angular resolution (0.4″: 600 AU, at the Bommerang's distance, 1.5 kpc [SN97]) (Fig. 2a,b). For the first time we can make a detailed match of the molecular-line structure of the lobes in a PPN to the structure seen in scattered light in the HST optical image, confirming the common interpretation of these as expanding, thin-walled cavities.

In spectra extracted from a $0.3'' \times 0.2''$ region in the waist-center as seen in the 3–2 ^{12}CO and ^{13}CO images, the velocity width (FWHM~ 5 kms) is signif cantly smaller than that in the bipolar outf ow (Fig. 2c), and the centroid of the ^{13}CO line is blue-shifted from that of the ^{12}CO line. This can be explained as the well-known radiative-transfer effect in an optically-thick expanding medium where the excitation temperature falls with radius (and may also require a velocity-gradient). A position-velocity cut of the ^{13}CO(3–2) intensity taken along the major axis of the waist has a morphology that is not a simple ellipse (as expected for expansion), and may contain a component due to Keplerian rotation. If true, then the central region of the Boomerang resembles the disk in the the Red Rectangle (a disk-prominent post-AGB object), that shows Keplerian rotation (expansion) in its inner (outer) regions (Bujarrabal et al. 2013). Higher angular-mapping with ALMA can easily test this possibility.

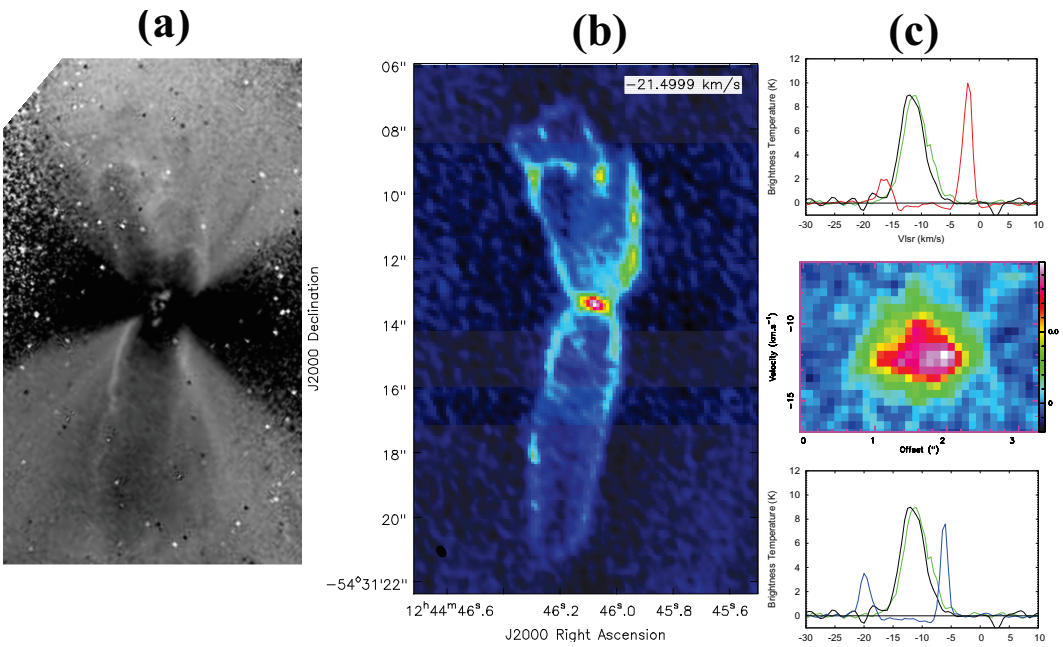

Figure 2. (a) HST 0.6μm polarized intensity (Cracraft & Sparks 2007), and (b) ALMA ^{12}CO(3–2) images of the central bipolar nebula in the Boomerang, (c) The top (bottom) panel shows ^{12}CO(3–2) spectra extracted from the northern (southern) lobe in red (blue), and the ^{12}CO and ^{13}CO 3–2 spectra from the central waist in green (scaled by 0.5) and black (scaled by 0.95); the center panel shows a position-velocity cut of the ^{13}CO(3–2) intensity, taken along the major axis of the waist.

We also f nd the unexpected presence of weak SO line (N,J=2,3-1,2) emission (Fig. 3a) towards the central region of the Boomerang; although noisy, the image indicates that the emission comes from the base of each bipolar lobe. The intrinsic line-width is 79 km s^{-1}, after deconvolving the limited spectral resolution of the continuum spectral window in which the line was found (15.625 MHz). Since SO is not expected to be present in the outf ows of C-rich AGB stars, our detection of SO in the Boomerang (which is C-rich) indicates that it results from a post-AGB process. A likely candidate is shock-driven chemistry, possibly involving dust sputtering that releases S locked up as solid MgS in grains (e.g., ISO observations show a strong 30 μm feature in C-rich evolved stars attributed to MgS: Hony et al. 2002).

2.2. Continuum Observations

We also observed the continuum emission at 3.3 and 0.88 mm towards the Boomerang. The waist shows a core-halo structure in the thermal dust emission at 0.88 mm. Modelling of the radio-to-(sub)millimeter-wave SED, including the cycle 0 and cycle 1 continuum measurements (Fig. 3b) show that the exponent of the dust absorption power-law (ν^p) is rather low ($p = 0.3$), conf rming the presence of about $5 \times 10^{-4}\ M_\odot$ of very large ($\gtrsim$mm-sized), cold (~30K) grains (Pap1) – comparable masses of large grains have also been found in the central regions of other PPNe and disk-prominent post-AGB objects (e.g., Sahai et al. 2011).

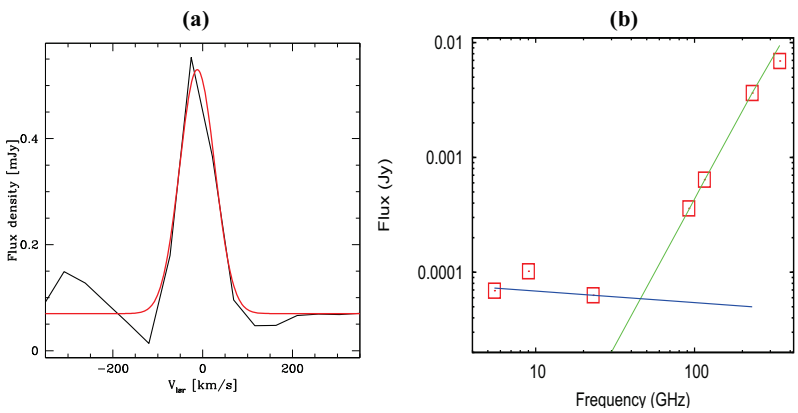

Figure 3. (a) SO line (N,J=2,3-1,2) emission from the Boomerang (red curve shows a Gaussian f t with FWHM=91.8 km s^{-1}) (b) The radio to millimeter-wave SED of the Boomerang. The radio measurements are upper limits. Green curve shows a f t to the mm-wave data with a shallow dust-emissivity power-law index, $p = 0.3$

In summary, our Cycle 1 observations of the Boomerang Nebula shed new light on extreme mass-ejection phenomena during the AGB and post-AGB phase of an intermediate-mass star, and highlight the need for (a) higher-angular resolution observations to search for rotation in the central region, and (b) continuum observations at $\lambda > 3.3$ cm to further probe the properties of the very large grains found in this object.

Acknowledgments. RS's contribution to the research described here was carried out at JPL, California Institute of Technology, under a contract with NASA. WV was supported by the ERC consolidator grant 614264.

References

Bujarrabal, V., Castro-Carrizo, A., Alcolea, J., et al. 2013, A&A, 557, L11
Cracraft, M. & Sparks, W.B. 2007, STScI ISR ACS 2007-10
Hony, S., Waters, L. B. F. M., & Tielens, A. G. G. M. 2002, A&A, 390, 533
Sahai, R., Claussen, M. J., Schnee, S., Morris, M., Sánchez Contreras, C. 2011, ApJ, 739, L3
Sahai, R., Morris, M., Sánchez Contreras, C., & Claussen, M. 2007, AJ, 134, 2200
Sahai, R., Morris, M. R., & Villar, G. G. 2011, AJ, 141, 134
Sahai, R. & Nyman, L-Å., 1997, ApJ, 487, L155 (SN97)
Sahai, R., Vlemmings, W. H. T., Huggins, P. J., Nyman, L.-Å., & Gonidakis, I. 2013, ApJ, 777, 92 (Pap1)